Published in final edited form as:
Science. 2012 March 23; 335(6075): 1496–1499. doi:10.1126/science.1214680.

MARF1 regulates essential oogenic processes in mice

You-Qiang Su[1], **Koji Sugiura**[1,*], **Fengyun Sun**[1], **Janice K. Pendola**[1], **Gregory A. Cox**[1], **Mary Ann Handel**[1], **John C. Schimenti**[2], and **John J. Eppig**[1,†]

[1]The Jackson Laboratory, Bar Harbor, ME 04609, USA

[2]College of Veterinary Medicine, Cornell University, Ithaca, NY 14853

Abstract

Development of fertilization-competent oocytes depends on integrated processes controlling meiosis, cytoplasmic development, and maintenance of genomic integrity. We show that meiosis arrest female 1 (MARF1) is required for these processes in mammalian oocytes. Mutations of *Marf1* cause female infertility characterized by up-regulation of a cohort of transcripts, increased retrotransposon expression, defective cytoplasmic maturation, and meiotic arrest. Up-regulation of protein phosphatase 2 catalytic subunit (PPP2CB) is key to the meiotic arrest phenotype. Moreover, *Iap* and *Line1* retrotransposon mRNAs are also up-regulated, and, concomitantly, DNA double-strand breaks are elevated in mutant oocytes. Therefore MARF1, by suppressing levels of specific transcripts, is an essential regulator of important oogenic processes leading to female fertility and the development of healthy offspring.

Oogenic processes essential for producing a "good" egg competent to support production of healthy offspring include accurate completion of meiosis (1), cytoplasmic maturational events that provide competence for fertilization and embryogenesis (1, 2), and maintenance of genomic integrity by protection against disruptive factors such as retrotransposon activation (3). Precise control of these processes is critical for successful reproduction, and abnormalities in any of these can lead to infertility, miscarriage and/or birth defects, and endanger future generations. We report here the discovery of a previously unknown "master" regulator in mouse oocytes that is required for all of these oogenic processes and acts by suppressing levels of specific transcripts.

Using ENU mutagenesis, we produced a line of mutant mice with a female-only autosomal recessive infertility phenotype (fig. S1) characterized initially by oocyte meiotic arrest; the mutation was designated ENU375-18. Mutant ovaries appeared normal (fig. S2A–C), but oocytes did not resume meiosis even after a superovulatory regimen of gonadotropins, and were ovulated at the immature germinal vesicle (GV) stage (Fig. 1A, fig. S2D). In contrast, both wild type (WT) and heterozygous (HET) oocytes were ovulated at mature metaphase II (MII) stage (Fig. 1A, fig. S2D). Therefore, the hallmark of infertility in mutant females is oocyte meiotic arrest at the GV stage.

†To whom correspondence should be addressed. John.Eppig@jax.org(J.J.E.).
*Current address: Laboratory of Applied Genetics, Graduate School of Agricultural and Life Sciences, University of Tokyo, Tokyo, Japan.

Supporting Online Material
www.sciencemag.org
Materials and Methods
figs. S1 to S10
Table S1 to S5
References (15–29)

Positional cloning of the mutated gene revealed a G-T transition at the 5'-splice donor site of the 16th intron of the *4921513D23Rik* gene (fig. S3A–C). This mutation causes the skipping of exon 16 during pre-mRNA splicing (fig. S3B, D) resulting in expression of negligible levels of exon 16 mRNA in mutant fully-grown oocytes (FGOs) (Fig. 1 B), and a frameshift in the coding sequence with creation of a premature stop codon (fig. S3B, E). The 4921513D23RIK protein was not detected in mutant FGOs by an antibody targeting its C-terminus (Fig. 1C). Only a trace amount of 5'- *4921513D23Rik* mRNA was detected in mutant FGOs by qRT-PCR (Fig. 1B). This may be caused by nonsense mediated decay of the truncated *4921513D23Rik* mRNA, suggesting that $4921513D23Rik^{ENU375\text{-}18}$ is unlikely to be a neomorph but rather an extreme hypomorph.

To verify that mutation of *4921513D23Rik* is responsible for the ENU-induced phenotype, we produced mice carrying a gene-trapped allele of $4921513D23Rik^{Gt(AS0671)Wtsi}$ (fig. S4A, B), and mice with heteroallelic combination of $4921513D23Rik^{Gt(AS0671)Wtsi}$ and $4921513D23Rik^{ENU375\text{-}18}$ ($4921513D23Rik^{Gt(AS0671)Wtsi/ENU375\text{-}18}$). No 4921513D23RIK protein was detected in FGOs of $4921513D23Rik^{Gt(AS0671)Wtsi/Gt(AS0671)Wtsi}$ or $4921513D23Rik^{Gt(AS0671)Wtsi/ENU375\text{-}18}$ mice (Fig. 1C), and both types of mice phenocopied $4921513D23Rik^{ENU375\text{-}18/ENU375\text{-}18}$ (fig. S4C–F). This non-complementation of the two alleles indicates that the $4921513D23Rik^{ENU375\text{-}18}$ allele contains the causative mutation underlying the ENU-induced infertile phenotype. Hereafter the *4921513D23Rik* gene will be referred to as Meiosis arrest female 1 *(Marf1)* and the $Marf1^{ENU375\text{-}18}$ allele as $Marf1^{ENU}$ and the gene-trapped allele as $Marf1^{GT}$.

Marf1 contains 27 exons that encode a 7,765-base pair (bp) mRNA and 1,736-amino acid (aa) peptide (fig. S5A). There is 86% amino acid identity between mouse and human MARF1. cDNA cloning and sequencing revealed that mouse oocytes express a unique variant of *Marf1* different from the isoform expressed in cumulus cells. This oocyte–specific variant lacks 537-bp nucleotides at the 3'-end of exon 3 (fig. S5B). By sequence analysis, MARF1 has 3 major domains: an N-terminal "LK-Nuc" domain belonging to the 5'→3' nuclease domain superfamily of proteins having RNase activity; two "RRM" domains; and a C-terminal tandem repeat of "LOTUS" or "OST-HTH" novel domains also present in *Drosophila* Oskar and mammalian tudor domain-containing proteins (TDRD) 5 and 7 (4, 5) (fig. S5C).

Marf1 mRNA is highly expressed in oocytes relative to other cell types (fig. S6A). There is ~60 fold higher expression of *Marf1* mRNA detected in oocytes than in granulosa cells (Fig. 2A, B). MARF1 protein is also expressed predominantly by oocytes, and barely detectable in granulosa cells (Fig. 2B). This was further confirmed by a β-galactosidase (GAL) reporter assay in $Marf1^{GT/GT}$ ovaries, with positive β-GAL staining in oocytes of follicles at all developmental stages but not in other ovarian cell types (Fig. 2C, fig. S6B). Moreover, the mutant meiotic arrest defect is oocyte-autonomous. $Marf1^{ENU/ENU}$ oocytes, when developed *in vivo* within reaggregated chimeric follicles composed of $Marf1^{ENU/+}$ somatic cells and $Marf1^{ENU/ENU}$ oocytes, displayed the meiotic arrest phenotype, whereas $Marf1^{ENU/+}$ oocytes acquired meiotic resumption competency when grown in reaggregated ovarian follicles composed of $Marf1^{ENU/ENU}$ somatic cells and $Marf1^{ENU/+}$ oocytes (Table S1).

High levels of cAMP, produced in normal FGOs, maintain meiotic arrest (see fig. S7 for diagram illustrating meiotic control in FGOs). However, alleviation of cAMP inhibition, through pharmacological (fig. S8A) or genetic approaches (fig. S8B–C) did not reverse meiotic arrest in $Marf1^{ENU/ENU}$ oocytes. Therefore, loss of MARF1 function affects processes downstream of relief from cAMP inhibition. No activation of oocyte maturation promoting factor (MPF) was detected in $Marf1^{ENU/ENU}$ oocytes after administration of hCG (fig. S9A), nor was there reduction of expression of key cell cycle regulators that activate

MPF, *Cdk1, Ccnb1, Cdc25a,b,c*, in *Marf1*$^{ENU/ENU}$ FGOs (fig. S9B). However, microinjection of mRNA encoding an active form of CDC25B into *Marf1*$^{ENU/ENU}$ FGOs reversed the meiotic arrest, with ~ 56% of injected oocytes resuming meiosis, of which ~42% progressed to MII with normal appearing spindles (Fig. 3A, B, fig. S9C), and activated MPF (Fig. 3C). Therefore, defects in oocytes caused by *Marf1* mutation lie upstream of MPF activation.

To further determine the mechanisms of meiotic arrest in *Marf1* mutant oocytes, we examined the *Marf1*$^{ENU/ENU}$ oocyte transcriptome using microarray analysis. A cohort of transcripts was markedly elevated in *Marf1*$^{ENU/ENU}$ FGOs, with 377 transcripts expressed ≥4 fold higher than in WT oocytes, and only 27 transcripts down-regulated to the same extent (Fig. 3D, Table S3–4). This increased transcript expression and/or stability is consistent with proposed RNase activity of MARF1. Post-transcriptional control is also indicated by a lack of difference in the levels of unprocessed hnRNA in mutant oocytes, despite dramatic increases in mRNAs (Fig. 3E).

We did not detect elevated levels of *Wee2* mRNA (fig. S9D); however, we found a profound, ~34-fold, up-regulation of *Ppp2cb* mRNA encoding the beta-isoform catalytic subunit of PPP2 (also known as PP2A) in *Marf1*$^{ENU/ENU}$ oocytes (Fig. 4A), and PPP2C protein was up-regulated ~50% in *Marf1* mutant oocytes (fig. S9E). Brief treatment of *Marf1* mutant oocytes with 2.5 μM okadaic acid (OA), an inhibitor of PPP2, was sufficient to reverse meiotic arrest in the majority (~70%) of *Marf1* mutant oocytes (Fig. 4B) and induce MPF activation (Fig. 3C). Moreover, micro-injection of *Marf1*$^{ENU/ENU}$ oocytes with *Ppp2cb* siRNA knocked down *Ppp2cb* mRNA by ~77% (fig. 9F), and induced about 46% GVB (Fig. 4C). Micro-injection with *Ppp2cb* morpholinos also induced GVB in ~43% of mutant oocytes (Fig. 4D). Therefore, up-regulation of *Ppp2cb* is a key to meiotic arrest in *Marf1* mutant oocytes, although other factors are not excluded. Indeed, microarray analysis also revealed elevation of other transcripts in mutant oocytes that could be related to the meiotic arrest phenotype. For example, GO analysis (http://proto.informatics.jax.org/prototypes/vlad-1.5/) indicates that ADNP, ADORA2B, and IMPDH2 participate in cyclic nucleotide production; HORMAD1 and MLH3 are meiotic proteins involved in synaptonemal complex assembly and recombination; CCNE1, CDK9, CDK19, CDKN2B, CSPP1, HEXIM1, ID2, ID3, PSMG2, and RAD9 participate in regulation of cell cycle processes; and CDK9, OBFC2A, UBE2V2, and YY1 are involved in DNA repair. Moreover, among elevated transcripts there is a high representation of those encoding proteins that participate in regulation of cellular metabolism and gene expression (Table S5). It is not known whether all of these transcripts are direct targets of regulation by MARF1 or whether some mRNA levels are abnormally high as a consequence of disruption of oogenic processes.

Consistent with the up-regulation of a cohort of transcripts potentially affecting oocyte development, after in-vitro insemination, there was no cleavage or embryonic development of the *Marf1* mutant oocytes induced to mature to metaphase II by micro-injection with mRNA encoding an active form of CDC25B (Fig. 4E, fig. S10A). Therefore, defects in *Marf1* mutant oocytes are not restricted to those that directly influence meiotic progression; they include those crucial for acquisition of competence to undergo fertilization and embryogenesis.

Surprisingly, steady-state levels of transcripts for intracisternal A particles (*Iap*) and long interspersed repetitive element (*Line*) 1 (but not other retrotransposons analyzed) were also significantly higher in *Marf1*$^{ENU/ENU}$ mutant oocytes than in WT (Fig. 4F). Retrotransposons exert deleterious effects on genomic integrity, in part because their dysregulated insertion into the genome produces DNA double-strand breaks (DSBs) (6).

Excess DSBs can affect meiotic progression in oocytes (7) and up-regulation of retrotransposons is associated with increased nuclear DSBs and meiotic arrest in mouse spermatocytes (8, 9). Therefore, the effect of *Marf1* mutations on nuclear DSBs was examined using γH2AX (also known as H2AFX) immunolabeling. The number of DSBs in both $Marf1^{ENU/ENU}$ and $Marf1^{GT/GT}$ mutant FGOs was significantly elevated compared to WT controls (Fig. 4G, fig. S10B). Increased DSBs may contribute to the meiotic arrest phenotype of *Marf1* mutant oocytes, as does over-expression of PPP2CB. In somatic cells, DSBs trigger G2/M checkpoints that inhibit entry of cells into mitosis. Interestingly, this checkpoint activation requires PPP2 and results in inhibition of CDC25 and subsequently CDK1 (10). It is unknown whether a similar mechanism regulates meiotic progression in mammalian oocytes because oocytes from mice carrying mutations that affect DSB repair usually die before follicular development (11). Although it is not clear whether the increase in nuclear DSBs directly affect meiosis, or activate a checkpoint control mechanism, MARF1 is the first protein known to be involved in establishing both retrotransposon mRNA levels and competence to resume meiosis in mammalian oocytes.

Together, these observations reveal a pivotal role for MARF1 in regulating oogenic processes essential for meiotic progression, genomic integrity, acquisition of developmental competence, and female fertility. The phenotype of meiotic arrest was a window through which other functions of this unique regulator were identified, and the mutant phenotypes are likely linked through up-regulation of mRNAs. Aberrant mRNA expression levels can be due to transcriptional or post-transcriptional control. Significantly, although MARF1 does not possess domains typical of transcription factors, it does contain a predicted RNase domain. The fact that hnRNA primary transcript levels are not affected in *Marf1* mutants while their respective mRNAs are elevated provides support for mis-regulation of transcript processing and/or stability, suggesting involvement of MARF1 in RNA homeostasis. Indeed, post-transcriptional control of RNA levels is emerging as a regulatory mechanism of considerable significance in germ cell development (12), and its involvement in oocyte meiotic progression has been demonstrated by analyses of oocyte-specific conditional knockouts of *Dicer1* (13, 14). Through its direct and indirect effects, MARF1 is clearly pivotal in establishing the network of pathways essential for the development of a “good” egg.

Supplementary Material

Refer to Web version on PubMed Central for supplementary material.

Acknowledgments

We thank Dr. M. Conti for providing the *Cdc25b* plasmid and $Gpr3^{-/-}$ mice, K. Wigglesworth and M. O’Brien for technical assistance. Supported by NIH grant HD42137 (Y.-Q.S., K.S., F.S., J.K.P., M.A.H., J.C.S., and J.J.E.) and Scientific Services by grant CA34196 from the NCI. Microarray data are deposited in the Gene Expression Omnibus (www.ncbi.nlm.nih.gov/geo, dataset GSE 31985).

References and Notes

1. Eppig JJ. Reprod. Fertil. Dev. 1996; 8:485. [PubMed: 8870074]
2. Swain JE, Pool TB. Hum. Reprod. Update. 2008; 14:431. [PubMed: 18603645]
3. Zamudio N, Bourc'his D. Heredity. 2010; 105:92. [PubMed: 20442734]
4. Anantharaman V, Zhang D, Aravind L. Biol. Direct. 2010; 5:13. [PubMed: 20302647]
5. Callebaut I, Mornon JP. Bioinformatics. 2010; 26:1140. [PubMed: 20305267]
6. Hedges DJ, Deininger PL. Mutat. Res. 2007; 616:46. [PubMed: 17157332]
7. Tatone C, et al. Hum. Reprod. 2011; 26:1843. [PubMed: 21558076]

8. Soper SF, et al. Dev. Cell. 2008; 15:285. [PubMed: 18694567]
9. Ma L, et al. PLoS Genet. 2009; 5:e1000635. [PubMed: 19730684]
10. Yan Y, et al. Oncogene. 2010; 29:4317. [PubMed: 20498628]
11. Di Giacomo M, et al. Proc. Natl. Acad. Sci. U. S. A. 2005; 102:737. [PubMed: 15640358]
12. Voronina E, Seydoux G, Sassone-Corsi P, Nagamori I. Cold Spring Harb. Perspect. Biol. 2011; 3:a002774. [PubMed: 21768607]
13. Murchison EP, et al. Genes Dev. 2007; 21:682. [PubMed: 17369401]
14. Tam OH, et al. Nature. 2008; 453:534. [PubMed: 18404147]

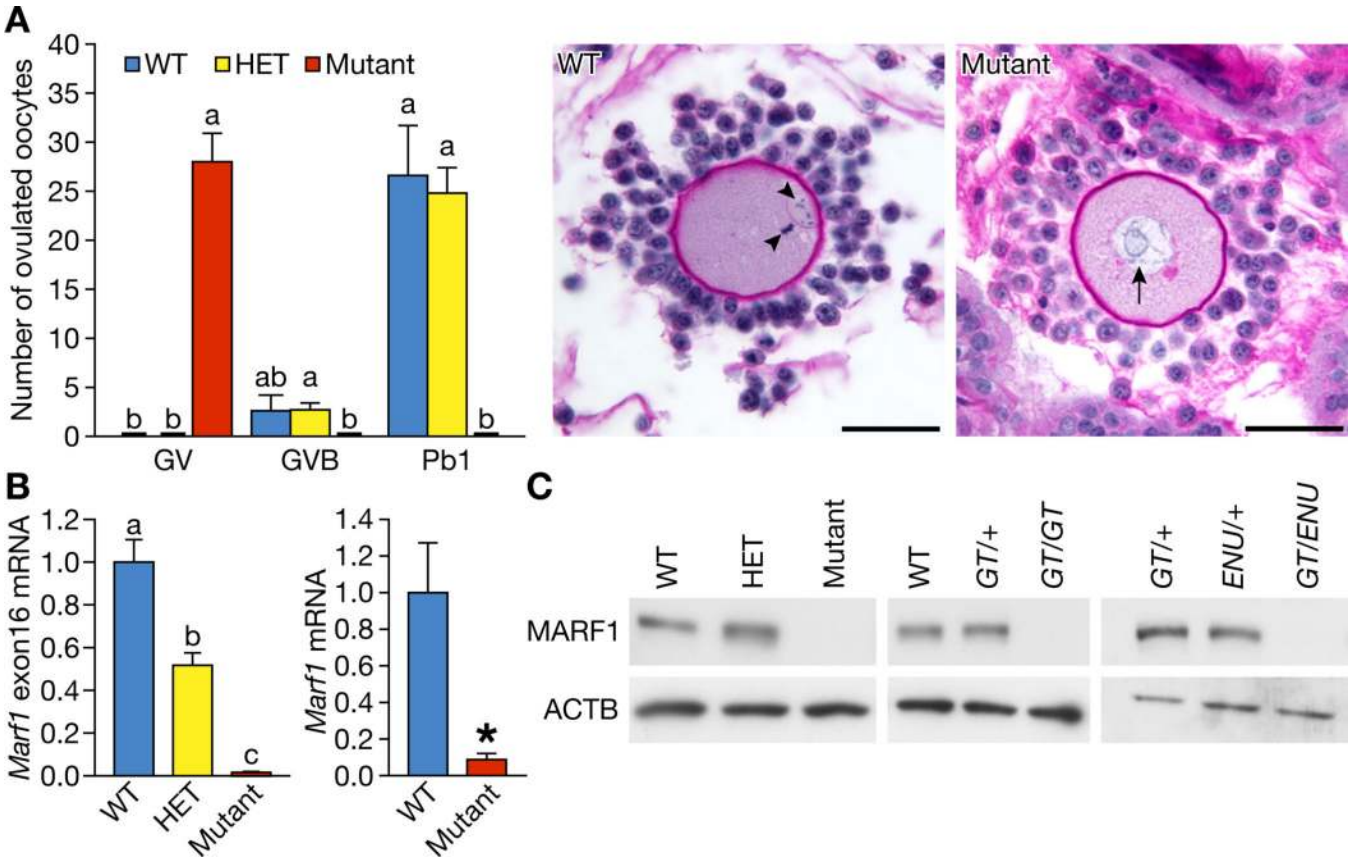

Fig. 1. Meiotic arrest and loss of *Marf1* expression in *Marf1* mutant oocytes

(A) Number of oocytes (left) and histology of cumulus-oocyte complexes (right) ovulated in oviducts by WT, HET, and mutant $Marf1^{ENU}$ females 14 h after hCG injection. GV: germinal vesicle; GVB: GV breakdown; Pb1: first polar body. Scale bars, 50 μm. Arrowheads indicate MII spindle and Pb1. Arrow indicates GV. **(B)** qRT-PCR of *Marf1* exon 16 (left) and 5'- (right) mRNA expression in WT, HET, and mutant $Marf1^{ENU}$ FGOs. In this and subsequent figures, graphs show mean ± SEM. *P<0.05, compared to WTs. Bars connected with different letters are significantly different, P<0.05. **(C)** Western blot of MARF1 and ACTB protein in WT, HET and mutant $Marf1^{ENU}$ FGOs (left), WT, HET (*GT/+*) and mutant $Marf1^{GT}$ (*GT/GT*) (middle), $Marf1^{GT/+}$ (*GT/+*), $Marf1^{ENU/+}$ (*ENU/+*) and $Marf1^{GT/ENU}$ (*GT/ENU*) (right panel).

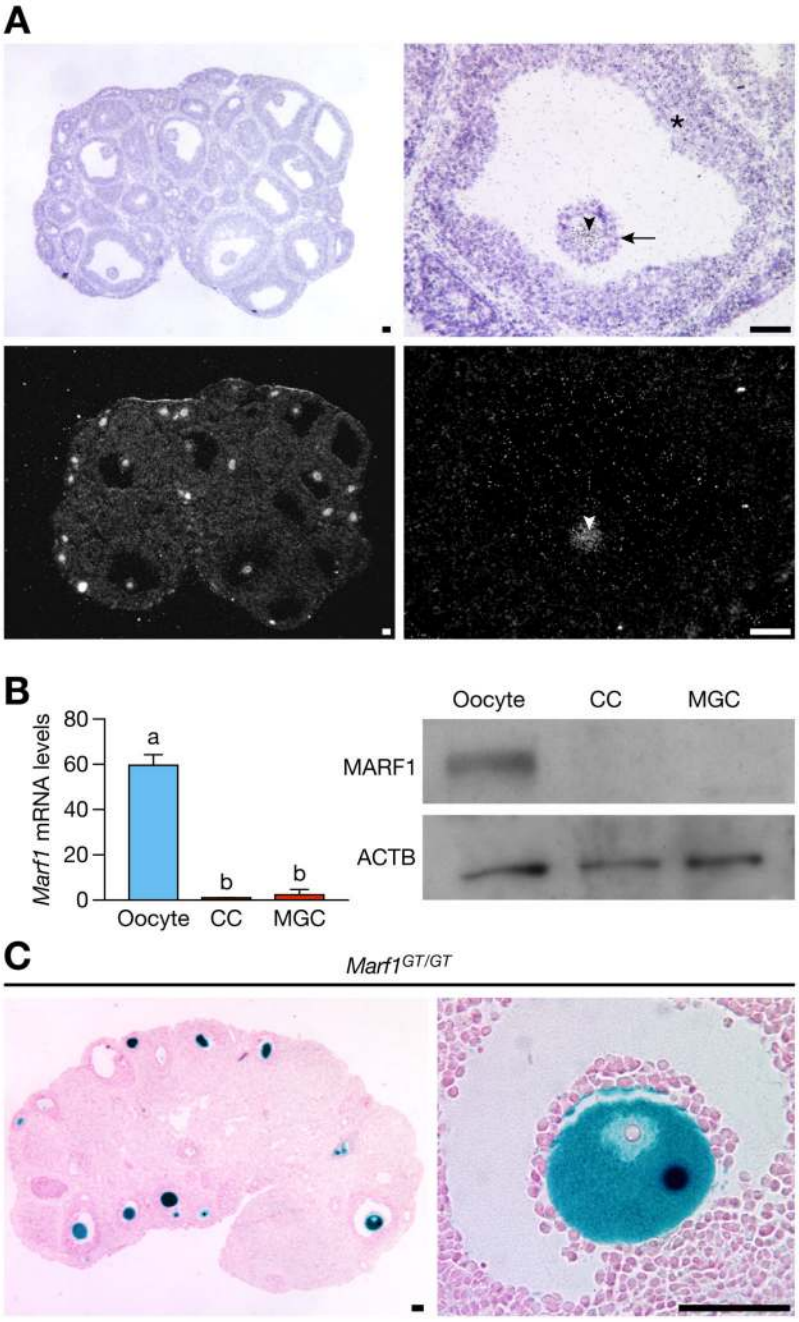

Fig. 2. Expression of *Marf1* by mouse oocytes

(A) *In situ* hybridization of *Marf1* mRNA in ovaries of 22-d old B6SJLF1 mice 46 h after eCG injection. Bright and dark field images are in the top and bottom panels, respectively. Arrowheads indicate oocytes, arrow indicates cumulus, and asterisk indicates mural granulosa cells. **(B)** qRT-PCR (left) and Western blot (right) analyses of *Marf1* mRNA and protein levels in oocytes, cumulus cells (CC), and mural granulosa cells (MGC) of eCG primed F1 mice. **(C)** X-gal staining of $Marf1^{GT/GT}$ ovaries from eCG (46 h) primed 22-d old mice. Scale bars, 50 μm.

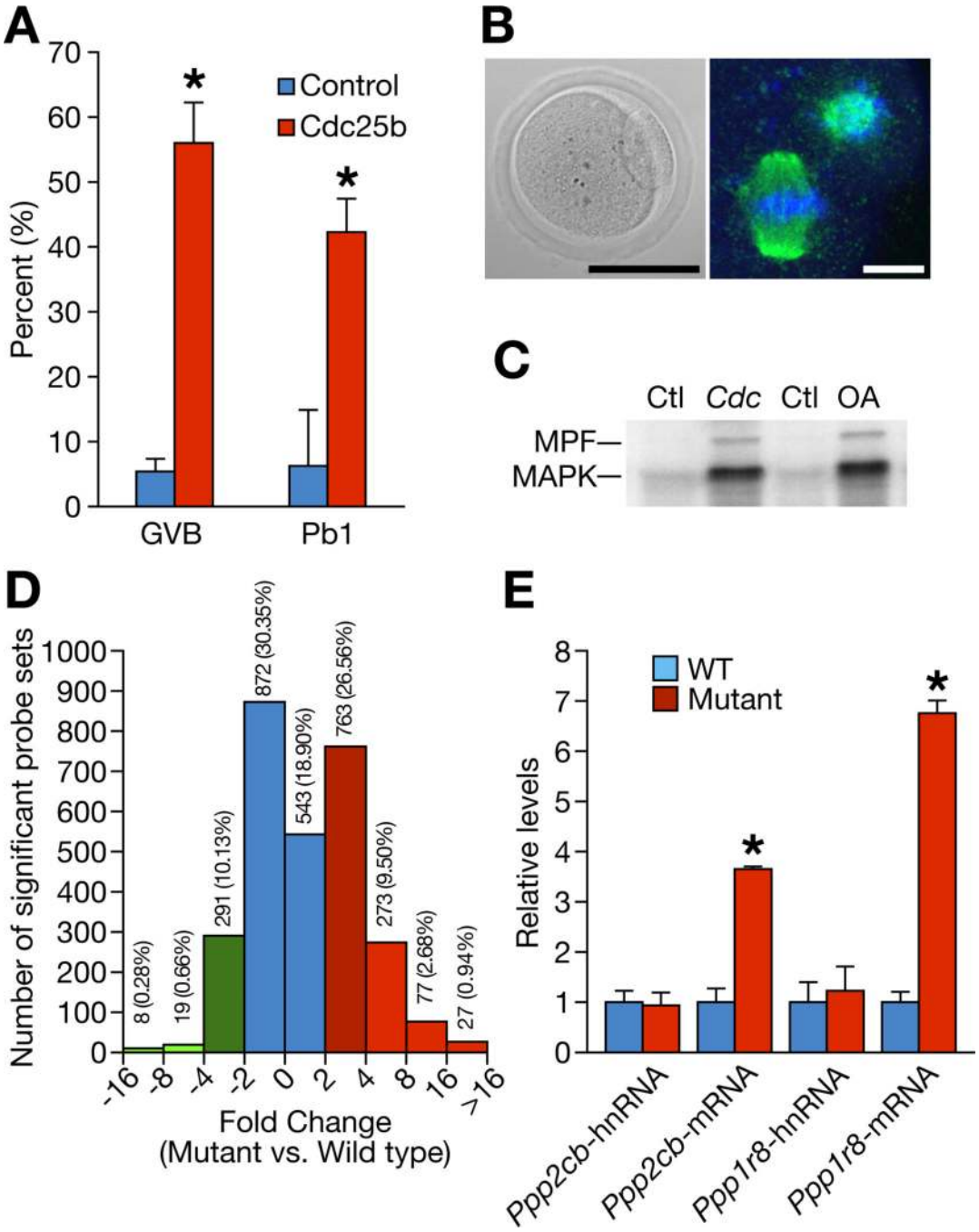

Fig. 3. Meiotic reversal by CDC25B and alteration of transcriptomes in *Marf1*$^{ENU/ENU}$ oocytes

(A) Effect of microinjection of *Cdc25b* mRNA (Cdc25b) on meiotic progression (GVB and Pb1 emission) in *Marf1*$^{ENU/ENU}$oocytes. **(B)** *Marf1*$^{ENU/ENU}$oocytes matured after *Cdc25b*-injection. Left: DIC image. Scale bar, 50 μm. Right: chromosomes (blue) and spindles (green) staining. Scale bar, 10 μm. **(C)** MPF and MAPK activity in *Marf1*$^{ENU/ENU}$oocytes with or without *Cdc25b* mRNA microinjection (*Cdc* and Ctl group, respectively), or treated with or without 2.5 μM okadaic acid (Ctl and OA group, respectively). **(D)** Distribution of significantly changed transcripts (represented by Affymetrix probe sets) at various magnitudes of difference in expression levels between *Marf1*$^{ENU/ENU}$ (Mutant) and WT

FGOs detected by microarray analysis. The number and the percentage of each group of transcripts in total changed transcripts are indicated above each bar. **(E)** Levels of heterogeneous nuclear RNA (hnRNA) and mRNAs measured by qRT-PCR in WT and *Marf1*$^{ENU/ENU}$ (Mutant) growing oocytes.

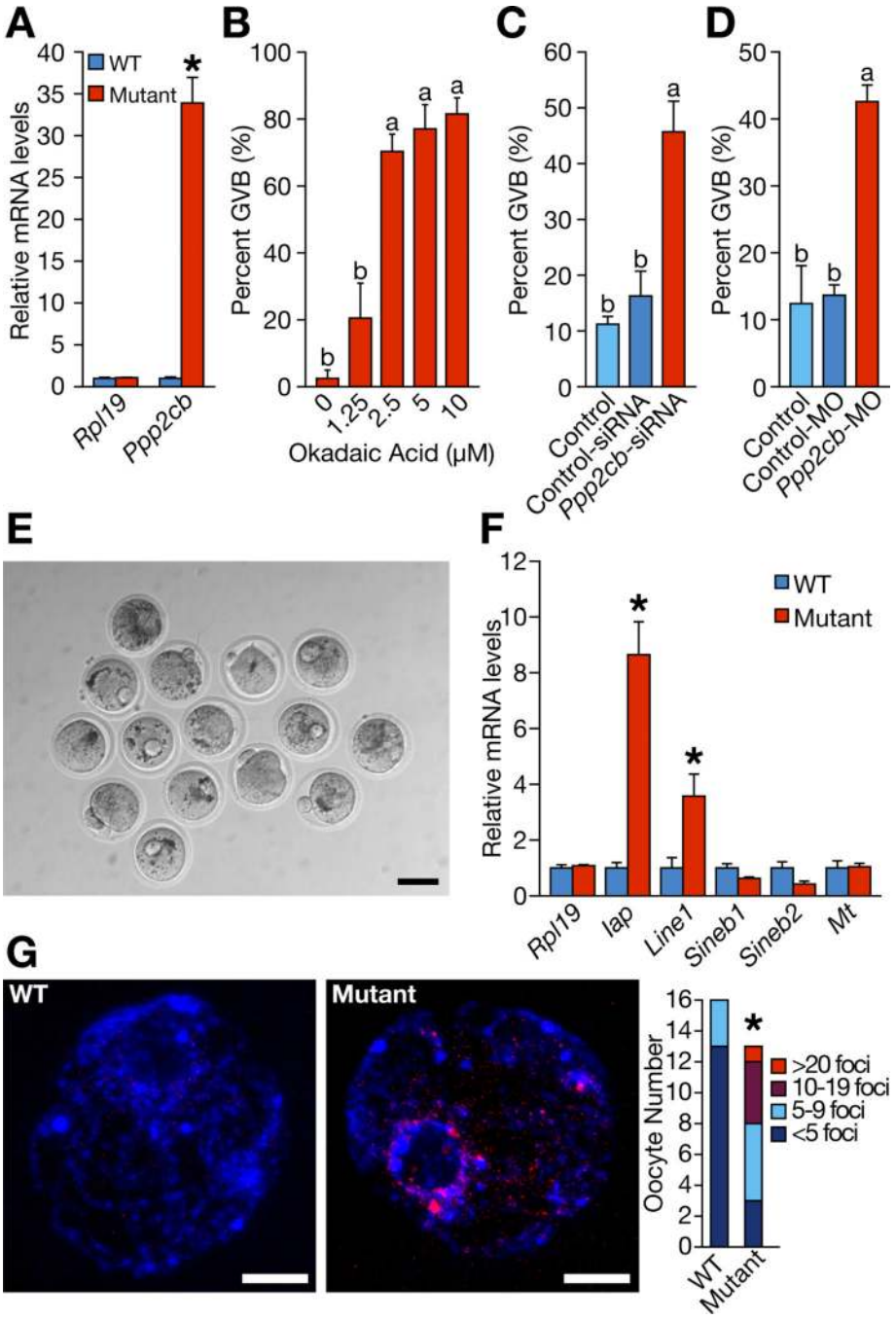

Fig. 4. Up-regulation of *Ppp2cb*, defective developmental competency, and dysregulation of retrotransposons and DNA double-strand breaks in *Marf1*$^{ENU/EMU}$ oocytes

(A) *Rpl19* and *Ppp2cb* mRNA expressed by WT and *Marf1*$^{ENU/ENU}$ (Mutant) FGOs. **(B)** Effect of okadaic acid on GVB in *Marf1*$^{ENU/ENU}$ FGOs. **(C–D)** Effect of microinjecting *Marf1*$^{ENU/ENU}$ FGOs with siRNAs **(C)** and morpholinos (MO) **(D)** on GVB. **(E)** Mature (induced by *Cdc25b*-injection) *Marf1*$^{ENU/ENU}$oocytes 24 h after IVF. Scale bar, 50 μm. **(F)** Levels of retrotransposon mRNAs measured by qRT-PCR in WT and *Marf1*$^{ENU/ENU}$ (Mutant) FGOs. **(G)** Confocal microscopy of FGOs stained with anti-γH2AX (red) and DAPI (blue). Scale bars, 5 μm. Bar graph shows the number of oocytes with various numbers of foci in the nucleus.